IEEE Access
Multidisciplinary | Rapid Review | Open Access Journal

SPECIAL SECTION ON EMERGING TRENDS, ISSUES AND CHALLENGES FOR ARRAY SIGNAL PROCESSING AND ITS APPLICATIONS IN SMART CITY

Received December 30, 2018, accepted January 19, 2019, date of publication January 24, 2019, date of current version February 12, 2019.

Digital Object Identifier 10.1109/ACCESS.2019.2894624

Three-Parallel Co-Prime Polarization Sensitive Array for 2-D DOA and Polarization Estimation via Sparse Representation

WEIJIAN SI, YAN WANG, AND CHUNJIE ZHANG
College of Information and Communication Engineering, Harbin Engineering University, Harbin 150001, China

Corresponding author: Chunjie Zhang (zhangchunjie@hrbeu.edu.cn)

This work was supported by in part by the National Natural Science Foundation of China under Grant 61671168 and Grant 61801143, in part by the Natural Science Foundation of Heilongjiang Province under Grant QC2016085, and in part by the Fundamental Research Funds for the Central Universities under Grant HEUCFJ180801 and Grant HEUCF180801.

ABSTRACT Co-prime array configurations are considered attractive due to the extension of degrees of freedom (DOFs) and the sparse placement of array elements. In this paper, a 2-D direction-of-arrival (DOA) and polarization estimation algorithm are proposed with the three-parallel co-prime polarization sensitive array which consists of the co-centered orthogonal loop and dipole. A novel cross-covariance matrix, that not contains the polarization parameters, is constructed to decouple the joint estimation problem of 2-D DOA angles and polarization parameters. Then, by using the vectorization operation and linear transformation, a virtual uniform linear array with larger DOFs is achieved. Meanwhile, a sparse representation-based algorithm is presented to estimate 2-D DOA angles with the only 1-D dictionary. To avoid the selection of regularization parameter in the sparse recovery process, we derive the constraint form of the optimization problem based on the upper bound of the data fitting error, which can reduce the effect of improper selection on regularization parameter. Finally, the polarization parameters are estimated via a least squares method. Since the proposed algorithm constructs the data vector with cross-covariance matrices between subarrays, the influence of noise is suppressed, and the estimation accuracy with low signal-to-noise ratio is enhanced. In the end, the simulation results demonstrate the effectiveness of the proposed algorithm.

INDEX TERMS Co-prime array configurations, direction-of-arrival estimation, polarization parameter estimation, polarization sensitive array, signal processing, sparse representation.

I. INTRODUCTION

The direction-of-arrival (DOA) estimation is a vital problem in the field of array signal processing [1]–[3], especially the estimation of two-dimensional (2-D) DOA and polarization parameters based on the polarization sensitive array (PSA) [4]–[6]. The PSA composed of vector sensors can measure the direction and polarization information of the electromagnetic wave signals, which offers better estimation accuracy, target classification, recognition performance, and anti-jamming capability [7]–[9]. Over the past few decades, by using the PSAs, various DOA and polarization parameter estimation algorithms have been proposed. References [10], [11] constructed the long-vector (LV) received data model of the electromagnetic wave signal, and proposed polarized MUSIC algorithm with multi-dimensional spectrum peak searching of DOA and polarization parameters. By using the spatial-, temporal-, and polarization-invariance, respectively, a series of polarized ESPRIT-based algorithms [12]–[14] was presented with low computational cost. The vector cross-product based algorithm [15]–[17] can estimate the parameters without ambiguity, where only a single six-component vector sensor is used. In general, the algorithms using PSA can make use of the vector structure of electromagnetic signal, achieving the improvement of estimation performance.

However, all aforementioned algorithms need compact placement of the array elements, and cannot handle the parameter estimation problem under the condition that the signal number is larger than the sensor number. The inter-element spacing limit of less than or equal to half a

wavelength restricts the estimation performance, whereas the sparse array has much more potential advantages [18], [19]. In recent years, a new type of array configuration called co-prime array (CPA) [20]–[23] which consists of two subarrays has been proposed for increasing the degrees of freedom (DOFs). By vectorizing the covariance matrix of the array received data, the CPA can obtain $O(MN)$ DOFs with only $O(M+N)$ physical sensors where M and N are co-prime numbers. As for the 2-D DOA estimation, the parallel co-prime array (PCPA) [24]–[26], three-parallel co-prime array (TPCPA) [27], and co-prime planar array (CPPA) [28]–[30] are constructed by vectorizing the cross-covariance matrix of multiple subarrays. The DOF extension deeply promotes the study of DOA estimation by using CPAs. The spatial smoothing technique based-MUSIC [31]–[33] algorithm is used to solve the correlation during the vectorization operation. Subsequently, the sparse representation (SR) framework based algorithms [34]–[37] with CPAs are developed to fully exploit the extended DOFs. In summary, by placing the sensors in co-prime configuration, the CPA notably increases the DOFs, thereby more signals can be detected. Meanwhile, the array aperture is expanded due to the sparse placement of array elements in CPAs, which would improve the estimation performance.

In this paper, we construct the three-parallel co-prime polarization sensitive array (TPCP-PSA), and propose a novel cross-covariance matrix based algorithm to estimate 2-D DOA angles and polarization parameters. By utilizing the received data of electric filed vector and magnetic field vector, we represent a new reconstructed cross-covariance matrix that not contains the polarization parameters. With the vectorization operation, a virtual uniform linear array (ULA) with $2M(N+1)-1$ DOFs was constructed. Then, the 2-D DOA angles are estimated by SR based method with only one-dimensional (1-D) overcomplete dictionary. Finally, the polarization parameters are obtained via least squares method. Compared with the current estimation algorithm based on PSA, the proposed algorithm increases the DOFs dramatically since the co-prime configuration is applied, which improves the estimation performance, and the underdetermined estimation case can be handled. Since it is hard to select a proper regularization parameter for the sparse recover method based on ℓ_1-norm minimization, we deduce the constraint form of the optimization problem with the upper bound of the data fitting error to avoid the selection of regularization parameter. The simulation results indicate that the proposed algorithm has superior estimation performance.

The remainder of this paper is organized as follows. The problem is formulated in Section 2. The 2-D DOA and polarization parameter estimation of the proposed algorithm are explicitly described in Section 3, and the advantages and innovations of the proposed algorithm are discussed in Section 4. The numerical simulations are conducted to validate the effectiveness of the proposed algorithm in Section 5. Finally, Section 6 concludes this paper.

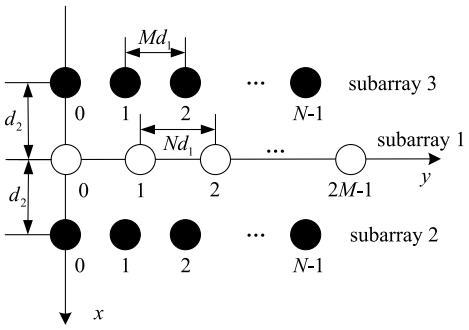

FIGURE 1. The planform of the three-parallel co-prime polarization sensitive array.

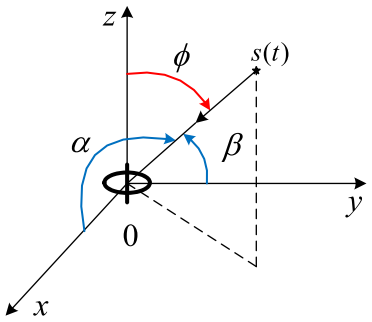

FIGURE 2. The structure of COLD sensor and the 2-D DOA angles of incident signal.

II. PROBLEM FORMULATION

A. THE THREE-PARALLEL CO-PRIME POLARIZATION SENSITIVE ARRAY

Consider a three-parallel co-prime polarization sensitive array consists of three uniform linear subarrays in the xoy-plane, as shown in Figure 1. The element herein is the co-centered orthogonal loop and dipole (COLD) and the dipole and loop both parallel to z-axis, as shown in Figure 2. The subarray 1 has $2M$ sensors with spacing Nd_1, both subarray 2 and 3 have N sensors with spacing Md_1, and the displacement spacing between the subarrays is d_2. The numbers M and N are co-prime, without loss of generality, assume that $M < N$, and $d_1 = d_2 \leq \lambda/2$ is a fundamental spacing.

B. THE ARRAY RECEIVED SIGNAL MODEL

Assume that K far-field and narrowband signals, which have travelled through a homogeneous isotropic medium, impinge on the array. Since the COLD sensor can only receive the z-component of electric field vector and magnetic field vector, the received part of the electromagnetic signal can be expressed in Cartesian coordinates as

$$\begin{bmatrix} e_{z,k} \\ h_{z,k} \end{bmatrix} = \begin{bmatrix} -\sin\phi_k \sin\gamma_k e^{j\eta_k} \\ -\sin\phi_k \cos\gamma_k \end{bmatrix} \tag{1}$$

where the ϕ_k denotes the elevation angle measured from the vertical z-axis, as shown in the Figure 2. $\gamma_k \in [0, \pi/2]$ and

$\eta_k \in [-\pi, \pi]$ denote the auxiliary polarization angle and the polarization phase difference, respectively. Then the received data model of the three subarrays can be expressed as

$$\boldsymbol{x}_1(t) = \begin{bmatrix} \boldsymbol{x}_{1,e}(t) \\ \boldsymbol{x}_{1,h}(t) \end{bmatrix} = \begin{bmatrix} \boldsymbol{A}_1(\beta)\boldsymbol{E}s(t) + \boldsymbol{n}_{1,e}(t) \\ \boldsymbol{A}_1(\beta)\boldsymbol{H}s(t) + \boldsymbol{n}_{1,h}(t) \end{bmatrix}, \tag{2}$$

$$\boldsymbol{x}_2(t) = \begin{bmatrix} \boldsymbol{x}_{2,e}(t) \\ \boldsymbol{x}_{2,h}(t) \end{bmatrix} = \begin{bmatrix} \boldsymbol{A}_2(\beta)\boldsymbol{\Phi}_2(\alpha)\boldsymbol{E}s(t) + \boldsymbol{n}_{2,e}(t) \\ \boldsymbol{A}_2(\beta)\boldsymbol{\Phi}_2(\alpha)\boldsymbol{H}s(t) + \boldsymbol{n}_{2,h}(t) \end{bmatrix}, \tag{3}$$

$$\boldsymbol{x}_3(t) = \begin{bmatrix} \boldsymbol{x}_{3,e}(t) \\ \boldsymbol{x}_{3,h}(t) \end{bmatrix} = \begin{bmatrix} \boldsymbol{A}_3(\beta)\boldsymbol{\Phi}_3(\alpha)\boldsymbol{E}s(t) + \boldsymbol{n}_{3,e}(t) \\ \boldsymbol{A}_3(\beta)\boldsymbol{\Phi}_3(\alpha)\boldsymbol{H}s(t) + \boldsymbol{n}_{3,h}(t) \end{bmatrix} \tag{4}$$

where (α, β) are the two-dimensional DOA angles, which denote the spatial angles measured from the positive x-axis and positive y-axis, respectively, as shown in the Figure 2. $\boldsymbol{s}(t)$ is the signal vector and $\boldsymbol{n}_{i,\varsigma}(t)(i = 1, 2, 3, \varsigma = e, h)$ is the complex noise vector. $\boldsymbol{A}_1(\beta) \in \mathbb{C}^{2M\times K}$ and $\boldsymbol{A}_2(\beta), \boldsymbol{A}_3(\beta) \in \mathbb{C}^{N\times K}$ are the spatial steering matrices of subarray 1, 2, and 3, the k-th columns are

$$a_1(\beta_k) = \left[1, e^{\mathrm{j}2\pi N d_1 \cos\beta_k/\lambda}, \cdots, e^{\mathrm{j}2\pi(2M-1)N d_1 \cos\beta_k/\lambda}\right]^{\mathrm{T}}, \tag{5}$$

$$\begin{aligned} a_2(\beta_k) &= a_3(\beta_k) \\ &= \left[1, e^{\mathrm{j}2\pi M d_1 \cos\beta_k/\lambda}, \cdots, e^{\mathrm{j}2\pi(N-1)M d_1 \cos\beta_k/\lambda}\right]^{\mathrm{T}} \end{aligned} \tag{6}$$

where $(\cdot)^{\mathrm{T}}$ denotes transpose operation. $\boldsymbol{\Phi}_2(\alpha)$ and $\boldsymbol{\Phi}_3(\alpha)$ are diagonal matrices and have the equation as

$$\boldsymbol{\Phi}_2(\alpha) = \boldsymbol{\Phi}_3^*(\alpha) = \mathrm{diag}\left(e^{\mathrm{j}2\pi d_2 \cos\alpha_1/\lambda}, \cdots, e^{\mathrm{j}2\pi d_2 \cos\alpha_K/\lambda}\right). \tag{7}$$

$\boldsymbol{E}$ and $\boldsymbol{H}$ are electric field and magnetic field matrices as

$$\boldsymbol{E} = \mathrm{diag}\left(e_{z,1}, \cdots, e_{z,K}\right), \tag{8}$$

$$\boldsymbol{H} = \mathrm{diag}\left(h_{z,1}, \cdots, h_{z,K}\right). \tag{9}$$

In addition, we make some assumptions as follows.

1) The received signal data is statistically independent among the sensors, dipoles and snapshots.
2) The complex noise is supposed to be temporally and spatially white Gaussian and uncorrelated with the sources.
3) There is no mutual coupling effect among the sensors and dipoles.

III. 2-D DOA ANGLE AND POLARIZATION PARAMETER ESTIMATION BASED ON SPARSE REPRESENTATION

A. TWO-DIMESIONAL DOA ESTIAMTION

In this subsection, the data vector of a virtual ULA is constructed to estimate the 2-D DOA angles by using the characteristic of co-prime numbers.

The cross-covariance matrix of $\varsigma(\varsigma = e, h)$-component of subarray 1 and 2 is

$$\boldsymbol{R}_{12,\varsigma} = E\left[\boldsymbol{x}_{1,\varsigma}(t)\boldsymbol{x}_{2,\varsigma}^{\mathrm{H}}(t)\right] = \boldsymbol{A}_1(\beta)\boldsymbol{S}_\varsigma\boldsymbol{\Phi}_2^*(\alpha)\boldsymbol{A}_2^{\mathrm{H}}(\beta) \tag{10}$$

where $\boldsymbol{S}_e = \boldsymbol{E}\boldsymbol{R}_s\boldsymbol{E}^{\mathrm{H}}$, $\boldsymbol{S}_h = \boldsymbol{H}\boldsymbol{R}_s\boldsymbol{H}^{\mathrm{H}}$, $\boldsymbol{R}_s = \mathrm{diag}(\sigma_1^2, \cdots, \sigma_K^2)$ is the covariance matrix of signal data, and σ_k^2 is the power of the k-th signal. The superscript $(\cdot)^{\mathrm{H}}$ denotes the complex conjugate transpose operation. The operator $E[\cdot]$ denotes the expectation operation. Then, define a new cross-covariance matrix as

$$\boldsymbol{R}_{12} = \boldsymbol{R}_{12,e} + \boldsymbol{R}_{12,h} = \boldsymbol{A}_1(\beta)\boldsymbol{S}\boldsymbol{\Phi}_2^*(\alpha)\boldsymbol{A}_2^{\mathrm{H}}(\beta) \tag{11}$$

where

$$\boldsymbol{S} = \boldsymbol{S}_e + \boldsymbol{S}_h = \mathrm{diag}\left(\sigma_1^2 \sin^2\phi_1, \cdots, \sigma_K^2 \sin^2\phi_K\right) \tag{12}$$

is a diagonal matrix. It is obviously that $\boldsymbol{R}_{12}$ only involves 2-D DOA angles but not the polarization parameters.

By using the vectorization operator, $\boldsymbol{R}_{12}$ can be transformed into a vector form as

$$\boldsymbol{r}_{12} = \mathrm{vec}(\boldsymbol{R}_{12}) = \boldsymbol{B}_{12}(\beta)\cdot\boldsymbol{p} \tag{13}$$

where $(\cdot)^*$ denotes conjugate operation, and

$$\boldsymbol{B}_{12}(\beta) = \boldsymbol{A}_2^*(\beta) \odot \boldsymbol{A}_1(\beta), \tag{14}$$

$$\begin{aligned} \boldsymbol{p} &= \mathrm{d}\left(\boldsymbol{S}\boldsymbol{\Phi}_2^*(\alpha)\right) \\ &= \left[\sigma_1^2 \sin^2\phi_1 e^{-\mathrm{j}2\pi d_2 \cos\alpha_1/\lambda}, \cdots, \right. \\ &\qquad \left. \sigma_K^2 \sin^2\phi_K e^{-\mathrm{j}2\pi d_2 \cos\alpha_K/\lambda}\right]^{\mathrm{T}} \end{aligned} \tag{15}$$

in which $\odot$ denotes the Khatri-Rao product, and $\mathrm{d}(\cdot)$ is the operator that forms a column vector with the diagonal elements of the diagonal array.

If $\boldsymbol{r}_{12}$ is regarded as a single snapshot data vector of a virtual line array (VLA), $\boldsymbol{B}_{12}(\beta)$ is the corresponding steering vector matrix, $\boldsymbol{p}$ is the single snapshot signal vector, and the virtual array elements are located at

$$\mathbb{L}_{12} = \left\{(x_{1,i} - x_{2,j})d_1 \,|0 \le i \le 2M-1, 0 \le j \le N\right\} \tag{16}$$

where $x_{1,i}$ is the location of the i-th physical sensor in the subarray 1, $x_{2,j}$ is the location of the j-th physical sensor in the subarray 2. It is easy to known that the locations of virtual array elements are not continuous and uniform. Benefiting from the characteristic of the co-prime numbers M and N, a virtual uniform linear array (VULA) consists of $M(N+1)$ virtual elements can be constructed, and the virtual array elements are located at

$$\tilde{\mathbb{L}}_{12} = \{ld_1 \,|0 \le l \le M(N+1) - 1\}. \tag{17}$$

Extract the entries of $\boldsymbol{r}_{12}$ and $\boldsymbol{B}_{12}(\beta)$ corresponding to the locations in $\tilde{\mathbb{L}}_{12}$, and the single snapshot data vector of VULA can be obtained as

$$\boldsymbol{z}_{12} = \boldsymbol{P}_{12}\boldsymbol{r}_{12} = \tilde{\boldsymbol{B}}_{12}(\beta)\cdot\boldsymbol{p} \tag{18}$$

where

$$\tilde{\boldsymbol{B}}_{12}(\beta) = \boldsymbol{P}_{12}\boldsymbol{B}_{12}(\beta) = \left[\tilde{\boldsymbol{b}}_{12}(\beta_1), \cdots, \tilde{\boldsymbol{b}}_{12}(\beta_K)\right] \tag{19}$$

is the steering vector matrix, and the k-th column is

$$\tilde{\boldsymbol{b}}_{12}(\beta_k) = \left[1, \mathrm{e}^{\mathrm{j}2\pi d_1 \cos\beta_k/\lambda}, \cdots, \mathrm{e}^{\mathrm{j}2\pi(M(N+1)-1)d_1 \cos\beta_k/\lambda}\right]^{\mathrm{T}}. \tag{20}$$

$\boldsymbol{P}_{12}$ is the selection matrix to extract and sort the entries of $\boldsymbol{r}_{12}$ to construct z_{12}. Once the co-prime numbers M, N are determined, the selection matrix $\boldsymbol{P}_{12}$ is determined and can be known.

Follow the above ideas, the cross-covariance matrix of $\varsigma(\varsigma = e, h)$-component of subarray 3 and 1 can be obtained as

$$\boldsymbol{R}_{31,\varsigma} = E\left[\boldsymbol{x}_{3,\varsigma}(t)\boldsymbol{x}_{1,\varsigma}^{\mathrm{H}}(t)\right] = \boldsymbol{A}_3(\alpha)\boldsymbol{\Phi}_3(\beta)\boldsymbol{S}_\varsigma\boldsymbol{A}_1^{\mathrm{H}}(\alpha). \quad (21)$$

The defined new cross-covariance matrix is

$$\boldsymbol{R}_{31} = \boldsymbol{R}_{31,e} + \boldsymbol{R}_{31,h} = \boldsymbol{A}_3(\beta)\boldsymbol{\Phi}_3(\alpha)\boldsymbol{S}\boldsymbol{A}_1^{\mathrm{H}}(\beta), \quad (22)$$

and the vector form is

$$\boldsymbol{r}_{31} = \mathrm{vec}(\boldsymbol{R}_{31}) = \boldsymbol{B}_{31}(\beta)\cdot\boldsymbol{p}_{31} \quad (23)$$

where

$$\boldsymbol{B}_{12}(\beta) = \left(\boldsymbol{A}_2^*(\beta)\odot\boldsymbol{A}_1(\beta)\right), \quad (24)$$

$$\boldsymbol{p}_{31} = \mathrm{d}\left(\boldsymbol{\Phi}_3(\alpha)\boldsymbol{S}\right). \quad (25)$$

Since subarray 2 and 3 are symmetric about the x-axis, the equations $\boldsymbol{\Phi}_3(\alpha) = \boldsymbol{\Phi}_2^*(\alpha)$ and $\boldsymbol{p}_{31} = \boldsymbol{p}$ are established.

Similarly, if $\boldsymbol{r}_{31}$ is regarded as a single snapshot data vector of a VLA, $\boldsymbol{B}_{31}(\beta)$ is the corresponding steering vector matrix, $\boldsymbol{p}$ is the single snapshot signal vector, and the virtual array elements are located at

$$\mathbb{L}_{31} = \left\{(x_{3,j} - x_{1,i})d_1 \,|0 \le i \le 2M-1, 0 \le j \le N\right\}. \quad (26)$$

Then, the VULA consists of $M(N+1)-1$ virtual elements can be constructed, and the virtual array elements are located at

$$\tilde{\mathbb{L}}_{31} = \{ld_1 \,|-(M(N+1)-1) \le l \le -1\}. \quad (27)$$

Extract the entries of $\boldsymbol{r}_{31}$ and $\boldsymbol{B}_{31}(\beta)$ corresponding to the locations in $\tilde{\mathbb{L}}_{12}$, and we can obtain the single snapshot data vector of VULA as

$$z_{31} = \boldsymbol{P}_{31}\boldsymbol{r}_{31} = \tilde{\boldsymbol{B}}_{31}(\beta)\cdot\boldsymbol{p} \quad (28)$$

where

$$\tilde{\boldsymbol{B}}_{31}(\beta) = \boldsymbol{P}_{31}\boldsymbol{B}_{31}(\beta) = \left[\tilde{\boldsymbol{b}}_{31}(\beta_1), \cdots, \tilde{\boldsymbol{b}}_{31}(\beta_K)\right] \quad (29)$$

is steering vector matrix, and the k-th column is

$$\tilde{\boldsymbol{b}}_{31}(\beta_k) = \left[\mathrm{e}^{-\mathrm{j}2\pi(M(N+1)-1)d_1\cos\beta_k/\lambda}, \cdots, \mathrm{e}^{-\mathrm{j}2\pi d_1\cos\beta_k/\lambda}\right]^{\mathrm{T}}. \quad (30)$$

$\boldsymbol{P}_{31}$ is the selection matrix to extract and sort the entries of $\boldsymbol{r}_{31}$ to construct z_{31}. Once the co-prime numbers M, N are determined, the selection matrix $\boldsymbol{P}_{31}$ is determined and can be known.

Further, combine the single snapshot data vectors $\boldsymbol{r}_{31}$ and $\boldsymbol{r}_{12}$, a VULA that contains $2M(N+1)-1$ virtual elements can be obtained, and the virtual array elements are located at

$$\begin{aligned}\tilde{\mathbb{L}} &= \tilde{\mathbb{L}}_{31} \cup \tilde{\mathbb{L}}_{12} \\ &= \{ld_1 \,|-(M(N+1)-1) \le l \le (M(N+1)-1)\}. \quad (31)\end{aligned}$$

The corresponding signal snapshot data vector is

$$z = \begin{bmatrix} z_{31} \\ z_{12} \end{bmatrix} = \begin{bmatrix} \tilde{\boldsymbol{B}}_{31}(\beta) \\ \tilde{\boldsymbol{B}}_{12}(\beta) \end{bmatrix}\cdot\boldsymbol{p} = \tilde{\boldsymbol{B}}(\beta)\boldsymbol{p}. \quad (32)$$

However, the vectorization operation in (13) and (23) would induce correlation between the incident signals, hence, the signal model (32) can be considered as a ULA receiving K correlated incident signals. Note that the DOFs are extended from the physical sensor number of the TPCP-PSA $2(M+N)$ to the virtual element number of the VULA $2M(N+1)-1$, so that the parameter estimation problem on the underdetermined condition can be solved. Moreover, the cross-covariance matrices of the physical subarrays are used in the process of constructing the VULA, thus the data vector contains no noise terms, and the effect of the noise are suppressed.

Due to the correlation of signals and only single available snapshot, the subspace-based DOA estimation algorithm cannot be applied. The sparse representation based DOA estimation algorithms can handle the correlated problem naturally, and can work properly even if the snapshot is insufficient. From (32), it can be seen that the steering vector matrix only contains one DOA angle β, hence, one-dimensional spatial grid in the β angle domain is needed. By discretizing the β angle domain, a sampling grid $(\bar{\beta}_1, \bar{\beta}_2, \cdots, \bar{\beta}_Q)$ with $Q \gg K$ is formed. Assume that the grid is dense enough so that the actual DOA angles $\{\beta_k\}_{k=1}^K$ only lie within the grids. To obtain denser grids with less computation complexity, the multiresolution grid refinement [38] can be applied. Then the data vector $\boldsymbol{z}$ can be sparsely represented as

$$\boldsymbol{z} = \boldsymbol{\Phi}(\bar{\beta})\cdot\boldsymbol{u} \quad (33)$$

where $\boldsymbol{\Phi} = [\tilde{\boldsymbol{b}}(\bar{\beta}_1), \tilde{\boldsymbol{b}}(\bar{\beta}_2), \cdots, \tilde{\boldsymbol{b}}(\bar{\beta}_Q)]$ is an overcomplete dictionary, and $\boldsymbol{u}$ is a K sparse coefficient vector with $u_q \neq 0$ if $\exists\bar{\beta}_q = \beta_k$ and $u_q = 0$ otherwise. Obviously, $\boldsymbol{\Phi}(\bar{\beta})$ depends on the DOA angle β, whereas $\boldsymbol{u}$ depends on the other DOA angle α and the signal power. Hence, the 2-D DOA angles can be obtained by solving the following ℓ_1-norm minimization problem

$$\min_{\hat{\boldsymbol{u}}} \left\|\boldsymbol{z} - \boldsymbol{\Phi}(\bar{\beta})\cdot\hat{\boldsymbol{u}}\right\|_2 + \mu\left\|\hat{\boldsymbol{u}}\right\|_1 \quad (34)$$

where $\|\cdot\|_2$ and $\|\cdot\|_1$ denote the ℓ_2- and ℓ_1-norm, representing the residual error of $\boldsymbol{z}$ and the sparsity of estimated $\hat{\boldsymbol{u}}$. μ is the regularization parameter that balance these two norms. A small regularization parameter corresponds to good fits to the data and smaller residuals. However, this would lead to pseudo peaks in the spectrum. A large regularization parameter makes the estimation results over simplistic and fails to fit the data well. Due to the importance of μ and the difficulty of selecting an appropriate μ, we derive another form of (34) to avoid such a problem.

In practice, since the cross-covariance matrices in (10) and (21) are unavailable, they are usually replaced by the sample cross-covariance matrices within finite snapshots, i.e.

$$\hat{\boldsymbol{R}}_{12,\varsigma} = \frac{1}{L}\sum_{t=1}^{L}\boldsymbol{x}_{1,\varsigma}(t)\boldsymbol{x}_{2,\varsigma}^{\mathrm{H}}(t), \quad (35)$$

$$\hat{\boldsymbol{R}}_{31,\varsigma} = \frac{1}{L}\sum_{t=1}^{L} \boldsymbol{x}_{3,\varsigma}(t)\boldsymbol{x}_{1,\varsigma}^{\mathrm{H}}(t) \tag{36}$$

where $\varsigma(\varsigma = e, h)$ denotes the components of electric field vector or magnetic field vector, and L denotes the snapshot number.

Define an augmented cross-covariance matrix of ς-component as

$$\hat{\boldsymbol{R}}_{\varsigma} = \left[\hat{\boldsymbol{R}}_{31,\varsigma}\ \hat{\boldsymbol{R}}_{12,\varsigma}\right] \tag{37}$$

and the vector form is

$$\hat{\boldsymbol{r}}_{\varsigma} = \mathrm{vec}\left(\hat{\boldsymbol{R}}_{\varsigma}\right) = \begin{bmatrix}\hat{\boldsymbol{r}}_{31,\varsigma} \\ \hat{\boldsymbol{r}}_{12,\varsigma}\end{bmatrix} \tag{38}$$

where $\hat{\boldsymbol{r}}_{31,\varsigma}$ and $\hat{\boldsymbol{r}}_{12,\varsigma}$ are the vector forms of $\hat{\boldsymbol{R}}_{31,\varsigma}$ and $\hat{\boldsymbol{R}}_{12,\varsigma}$, respectively.

In accordance with [25], the estimation error $\Delta\boldsymbol{r}_{31,\varsigma}$ and $\Delta\boldsymbol{r}_{12,\varsigma}$ satisfy the asymptotic complex Gaussian distribution, i.e.

$$\Delta\boldsymbol{r}_{12,\varsigma} = \hat{\boldsymbol{r}}_{12,\varsigma} - \boldsymbol{r}_{12,\varsigma} \sim \mathrm{AsN}\left(0, \frac{1}{L}\left(\boldsymbol{R}_{2,\varsigma}^{\mathrm{T}} \otimes \boldsymbol{R}_{1,\varsigma}\right)\right), \tag{39}$$

$$\Delta\boldsymbol{r}_{31,\varsigma} = \hat{\boldsymbol{r}}_{31,\varsigma} - \boldsymbol{r}_{31,\varsigma} \sim \mathrm{AsN}\left(0, \frac{1}{L}\left(\boldsymbol{R}_{1,\varsigma}^{\mathrm{T}} \otimes \boldsymbol{R}_{3,\varsigma}\right)\right). \tag{40}$$

Therefore, the estimation error $\Delta\boldsymbol{r}_{\zeta}$ of the vector form of the augmented cross-covariance matrix also satisfies the asymptotic complex Gaussian distribution, i.e.

$$\Delta\boldsymbol{r}_{\varsigma} = \hat{\boldsymbol{r}}_{\varsigma} - \boldsymbol{r}_{\varsigma} \sim \mathrm{AsN}\left(0, \boldsymbol{C}_{\varsigma}\right) \tag{41}$$

with

$$\boldsymbol{C}_{\varsigma} = \frac{1}{L}\begin{bmatrix} \boldsymbol{R}_{1,\varsigma}^{\mathrm{T}} \otimes \boldsymbol{R}_{3,\varsigma} & \boldsymbol{R}_{21,\varsigma}^{\mathrm{T}} \otimes \boldsymbol{R}_{31,\varsigma} \\ \boldsymbol{R}_{13,\varsigma}^{\mathrm{T}} \otimes \boldsymbol{R}_{12,\varsigma} & \boldsymbol{R}_{2,\varsigma}^{\mathrm{T}} \otimes \boldsymbol{R}_{1,\varsigma} \end{bmatrix} \tag{42}$$

where $\boldsymbol{R}_{mn,\varsigma}$ is the cross-covariance matrix of subarray m and n at ς-component, and $\boldsymbol{R}_{m,\varsigma}$ is the auto-covariance matrix of subarray m at ς-component (See "Appendix" for the calculations of mean and variance of $\Delta\boldsymbol{r}_{\varsigma}$).

Further, according to the property of asymptotic complex Gaussian distribution, the estimation error of $\hat{\boldsymbol{r}} = \hat{\boldsymbol{r}}_e + \hat{\boldsymbol{r}}_h$ still satisfies the asymptotic complex Gaussian distribution, i.e.

$$\Delta\boldsymbol{r} = \hat{\boldsymbol{r}} - \boldsymbol{r} \sim \mathrm{AsN}\left(0, \boldsymbol{C}\right) \tag{43}$$

where $\boldsymbol{C} = \boldsymbol{C}_e + \boldsymbol{C}_h$.

From (32), the signal snapshot data vector can also be written as

$$\boldsymbol{z} = \begin{bmatrix}\boldsymbol{z}_{31} \\ \boldsymbol{z}_{12}\end{bmatrix} = \begin{bmatrix}\boldsymbol{P}_{31} & \\ & \boldsymbol{P}_{12}\end{bmatrix} \cdot \begin{bmatrix}\boldsymbol{r}_{31} \\ \boldsymbol{r}_{12}\end{bmatrix} = \boldsymbol{P} \cdot \boldsymbol{r}. \tag{44}$$

On the basis of [39], the estimation error of $\boldsymbol{z}$ satisfies

$$\Delta\boldsymbol{z} \sim \mathrm{AsN}\left(0, \boldsymbol{P}^{\mathrm{T}}\boldsymbol{C}\boldsymbol{P}\right). \tag{45}$$

Define the weight matrix

$$\boldsymbol{W} = \boldsymbol{P}^{\mathrm{T}}\boldsymbol{C}\boldsymbol{P}, \tag{46}$$

and normalize $\Delta\boldsymbol{z}$, then (45) can be derived as

$$\boldsymbol{W}^{-\frac{1}{2}}\Delta\boldsymbol{z} \sim \mathrm{AsN}\left(0, \boldsymbol{I}_{2M(N+1)-1}\right) \tag{47}$$

where $\boldsymbol{W}^{-\frac{1}{2}}$ is the Hermitian square root of $\boldsymbol{W}^{-1}$. Then, we can get that

$$\left\|\boldsymbol{W}^{-\frac{1}{2}}\Delta\boldsymbol{z}\right\|_2^2 \sim \mathrm{As}\chi^2\left(2M(N+1)-1\right) \tag{48}$$

where $\mathrm{As}\chi^2\left(2M(N+1)-1\right)$ denotes the asymptotic chi-square distribution with the DOF of $2M(N+1)-1$. From the analysis above, now the optimization problem in (34) is transformed to a constraint form as

$$\begin{aligned} &\min \ \ \left\|\hat{\boldsymbol{u}}\right\|_1 \\ &\text{s.t.} \ \ \left\|\hat{\boldsymbol{W}}^{-\frac{1}{2}}\left(\hat{\boldsymbol{z}} - \boldsymbol{\Phi}(\bar{\beta})\hat{\boldsymbol{u}}\right)\right\|_2 \le \sqrt{\xi} \end{aligned} \tag{49}$$

where $\hat{\boldsymbol{W}} = \boldsymbol{P}^{\mathrm{T}}\hat{\boldsymbol{C}}\boldsymbol{P}$ is the approximate weight matrix within finite snapshots. ξ is the acceptable upper bound of the fitting error, and it can be obtained with

$$\xi = \mathrm{chi2inv}\left(1-p, 2M(N+1)-1\right) \tag{50}$$

where chi2inv$(\cdot)$ is the inverse cumulative distribution function (in Matlab software) that makes the inequality in (49)holds with probability of $1-p$. Generally, it is enough to set $p = 0.001$ to make it nearly a sure event. The optimization problem is actually a second-order cone program (SOCP) [40] problem, and can be efficiently solved by off-the-shelf optimization software package such as CVX and SeDuMi. Therefore, the DOA estimation problem turns out to be that of recovering the K sparse vector $\boldsymbol{u}$. The locations of nonzero entries in $\boldsymbol{u}$ gives the estimations of DOA angle $\{\hat{\beta}_k\}_{k=1}^{K}$, and estimations of another DOA angle $\{\hat{\alpha}_k\}_{k=1}^{K}$ can be obtained from the values of nonzero entries via

$$\alpha_k = \arccos(-\lambda\arg(\hat{\boldsymbol{u}}_k)/2\pi d_2) \tag{51}$$

where $\hat{\boldsymbol{u}}_k$ is the k-th nonzero entries of the sparse vector $\hat{\boldsymbol{u}}$. It can be seen from (51) that the $\hat{\alpha}_k$ and $\hat{\beta}_k$ are estimated corresponding to the same entry in $\hat{\boldsymbol{u}}_k$, thus 2-D DOA are automatically paired.

B. POLARIZATION PARAMETER ESTIMATION

In this subsection, the polarization parameter estimated based on the estimation result of the DOA angles. According to subsection III-A, we can construct the data vectors as

$$\boldsymbol{z}_e = \left[\boldsymbol{z}_{31,e}^{\mathrm{T}}\ \boldsymbol{z}_{12,e}^{\mathrm{T}}\right]^{\mathrm{T}} = \tilde{\boldsymbol{B}}(\beta)\boldsymbol{p}_e, \tag{52}$$

$$\boldsymbol{z}_h = \left[\boldsymbol{z}_{31,h}^{\mathrm{T}}\ \boldsymbol{z}_{12,h}^{\mathrm{T}}\right]^{\mathrm{T}} = \tilde{\boldsymbol{B}}(\beta)\boldsymbol{p}_h, \tag{53}$$

$$\boldsymbol{z}_{eh} = \left[\boldsymbol{z}_{31,eh}^{\mathrm{T}}\ \boldsymbol{z}_{12,eh}^{\mathrm{T}}\right]^{\mathrm{T}} = \tilde{\boldsymbol{B}}(\beta)\boldsymbol{p}_{eh}, \tag{54}$$

$$\boldsymbol{z}_{he} = \left[\boldsymbol{z}_{31,he}^{\mathrm{T}}\ \boldsymbol{z}_{12,he}^{\mathrm{T}}\right]^{\mathrm{T}} = \tilde{\boldsymbol{B}}(\beta)\boldsymbol{p}_{he} \tag{55}$$

where $\boldsymbol{z}_{eh}$ and $\boldsymbol{z}_{he}$ are constructed by using the cross-covariance matrices between the electric field and magnetic field vector components of subarray 1 and that of

TABLE 1. The array information of the algorithms.

Algorithm	Array Configuration	M	N	DOF	Sensor Type
Proposed	TPCPA	3	4	29	COLD
TPCPA	TPCPA	3	4	29	Scalar Sensor
PCPA	PCPA	3	8	27	Scalar Sensor
LV-MUSIC	TPCPA	3	4	14	COLD

The array configuration of TPCPA refers to the three-parallel co-prim array, as shown in the Figure 1, and PCPA refers to the parallel co-prime array in [22].

subarray 2 and 3. $\boldsymbol{p}_e, \boldsymbol{p}_h, \boldsymbol{p}_{eh}, \boldsymbol{p}_{he}$ are all column vectors and the k-th entries are

$$\boldsymbol{p}_{e,k} = \sigma_k^2 \sin^2\phi_k \sin^2\gamma_k e^{-\mathrm{j}2\pi d_2 \cos\alpha_k/\lambda}, \tag{56}$$

$$\boldsymbol{p}_{h,k} = \sigma_k^2 \sin^2\phi_k \cos^2\gamma_k e^{-\mathrm{j}2\pi d_2 \cos\alpha_k/\lambda}, \tag{57}$$

$$\boldsymbol{p}_{eh,k} = \sigma_k^2 \sin^2\phi_k \sin\gamma_k \cos\gamma_k e^{\mathrm{j}\eta} e^{-\mathrm{j}2\pi d_2 \cos\alpha_k/\lambda}, \tag{58}$$

$$\boldsymbol{p}_{he,k} = \sigma_k^2 \sin^2\phi_k \sin\gamma_k \cos\gamma_k e^{-\mathrm{j}\eta} e^{-\mathrm{j}2\pi d_2 \cos\alpha_k/\lambda}. \tag{59}$$

By utilizing the estimations of the DOA angle $\{\hat{\beta}_k\}_{k=1}^K$, they can be estimated via least squares method as

$$\hat{\boldsymbol{p}}_e = \left(\tilde{\boldsymbol{B}}(\beta)\right)^{\dagger} z_e, \tag{60}$$

$$\hat{\boldsymbol{p}}_h = \left(\tilde{\boldsymbol{B}}(\beta)\right)^{\dagger} z_h, \tag{61}$$

$$\hat{\boldsymbol{p}}_{eh} = \left(\tilde{\boldsymbol{B}}(\beta)\right)^{\dagger} z_{eh}, \tag{62}$$

$$\hat{\boldsymbol{p}}_{he} = \left(\tilde{\boldsymbol{B}}(\beta)\right)^{\dagger} z_{he} \tag{63}$$

where $(\cdot)^{\dagger}$ denotes the pseudo-inverse of matrix. Then, the polarization parameter estimation results can be obtained via

$$\hat{\gamma}_k = \arctan\left(\sqrt{\frac{\hat{\boldsymbol{p}}_{e,k}}{\hat{\boldsymbol{p}}_{h,k}}}\right), \tag{64}$$

$$\hat{\eta}_k = \frac{1}{2}\mathrm{angle}\left(\frac{\hat{\boldsymbol{p}}_{eh,k}}{\hat{\boldsymbol{p}}_{he,k}}\right). \tag{65}$$

Obviously, the polarization parameter estimations $\{\hat{\gamma}_k\}_{k=1}^K$ and $\{\hat{\eta}_k\}_{k=1}^K$ are automatically paired with the 2-D DOA angles $\{\hat{\alpha}_k\}_{k=1}^K$ and $\{\hat{\beta}_k\}_{k=1}^K$.

C. ALGORITHM SUMMARY

So far, the two-dimensional DOA angles and polarization parameters are estimated based on the sparse representation of the cross-covariance matrices by using the three-parallel co-prime polarization sensitive array, and no parameter pair matching process is required. The major steps of the proposed algorithm are summarized as follows.

1) Compute the cross-covariance matrices $\boldsymbol{R}_{12}$ and $\boldsymbol{R}_{31}$ via (11) and (22) by using the electric and magnetic field vector components of subarray 1, 2 and 3, and get the vector forms through vectorization operation.

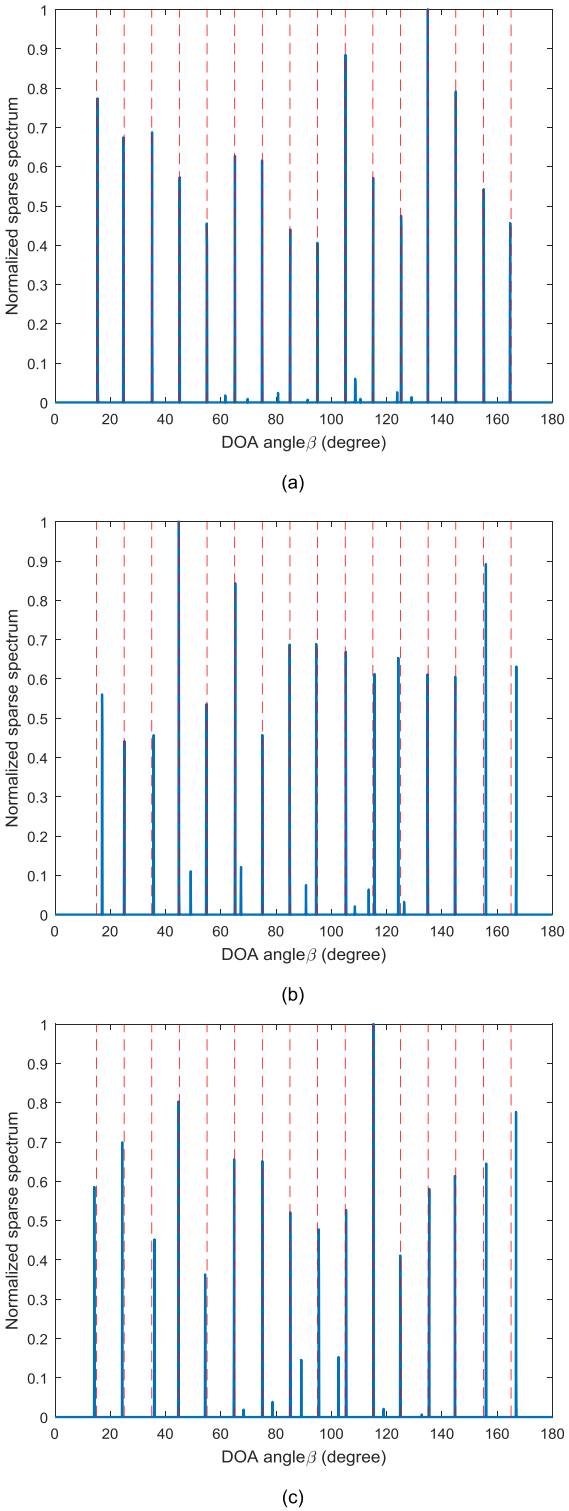

FIGURE 3. The spatial spectrums of (a) the proposed algorithm, (b) the TPCPA algorithm, and (c) the PCPA algorithm with SNR=0dB and 300 snapshots.

2) Obtain the selection matrices $\boldsymbol{P}_{12}$ and $\boldsymbol{P}_{31}$ according to the property of co-prime numbers M, N. Construct two virtual ULA, and get the data vectors z_{12} and z_{31} via (18) and (28). Then, combine these two data vectors via

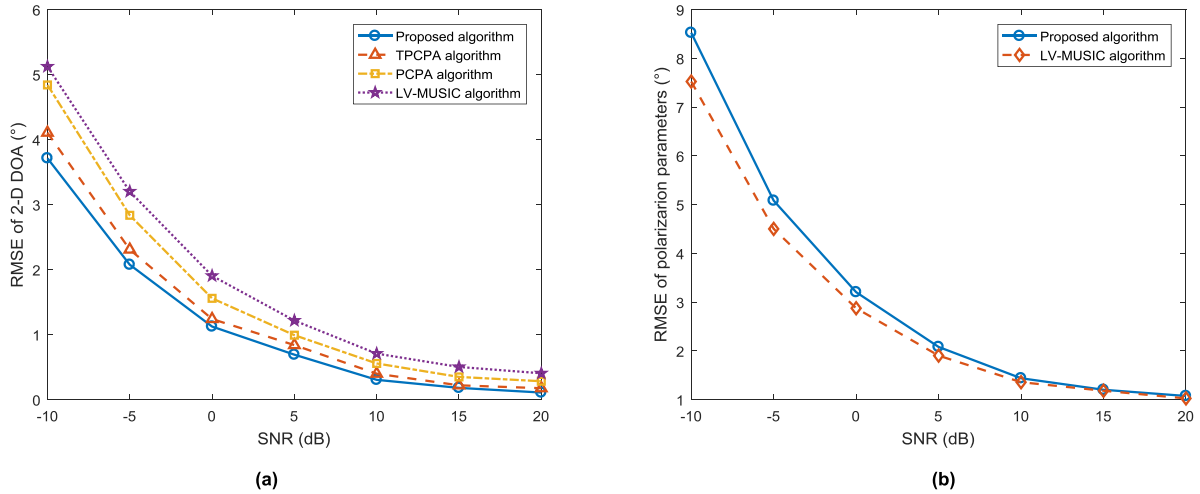

FIGURE 4. The RMSEs of (a) 2-D DOA angles and (b) polarization parameters versus SNR with 300 snapshots.

(32) and get the data vector z of the final virtual ULA which contains $2M(N+1)-1$ elements.

3) Discretizing the β angle domain to get the sampling grid, calculate the overcomplete dictionary $\mathbf{\Phi}(\bar{\beta})$ and represent z as the sparse representation as (33).
4) Compute the weight matrix $\hat{\boldsymbol{W}}$ and the upper bound of estimation error ξ via (46) and (50), respectively, and solve the optimization problem in (49), hence the 2-D DOA estimation results can be obtained.
5) Construct data vectors in (52) to (55), estimate coefficient vectors in (60) to (63) by using the least squares method, and calculate the polarization parameters via (64) and (65).

IV. DISCUSSIONS

The proposed algorithm introduces the co-prime array configuration into the polarization sensitive array, and presents the three-parallel co-prime polarization sensitive array to estimate the 2-D DOA and polarization parameters. This allows the proposed algorithm to estimate parameters on the underdetermined condition when the signals more than the array elements relative to the compact PSAs. On the other hand, compared with scalar co-prime array, the TPCP-PSA can measure the incident signals with vector structure, which achieves polarization parameter estimation and has better estimation performance.

By utilizing the characteristic of the co-prime number M and N, a virtual uniform linear array containing more array elements is constructed based on the cross-covariance matrices, and the observation data vector z can be obtained. According to (32), 2-D DOA angles are separated into two parts of the data vector, and the dictionary $\mathbf{\Phi}(\bar{\beta})$ in (33) can be easily constructed by sampling only 1-D DOA angle. Compared with the traditional SR-based 2-D DOA estimation algorithms, the dimension of the dictionary used in the sparse recover process is reduced from two to one, and the computation amount is decreased from $O((Q_1Q_2)^3)$ to $O(Q_1)^3$, where Q_1 and Q_2 are the grid number in each angle domain. In addition, due to the utilization of the cross-covariance matrices, there are no noise terms in the date vector, and the estimation accuracy with low SNR is improved.

Moreover, when estimating DOA angles, the constrained form of the optimization problem is derived. The acceptable upper bound of the data fitting error can be calculated with a large probability, then, the 2-D DOA can be obtained via sparse recover method. This eliminates the necessity of the regularization parameter selection and reduces the estimation performance loss due to the improper selection.

V. SIMULATIONS

In this section, a series of numerical simulations under different conditions are conducted to investigate the estimation performance of the proposed algorithm. The results are compared with PCPA algorithm [22], TPCPA algorithm [27], and LV-MUSIC algorithm [10]. The sensor number is set to be 14. The information of physical array used in the simulation is shown in the Table 1.

In the first simulation, we compare the spatial spectrums of the DOA angle β under the underdetermined condition. Assume there are $K = 16$ far-field narrowband signals impinging on the array. The DOA angle β are distributed within 15° to 165° with step of 10°, the DOA angle α are distributed within 80° to 10° and 170° to 100° with step of $-10°$, the auxiliary polarization angle γ and the polarization phase difference η are randomly distributed within the ranges of $(-90°, 90°)$ and $(-180°, 180°)$, respectively. The uniform spatial grid in β angle domain is formed with interval of 0.1°. The regularization parameters are 1.3 and 0.3 for TPCPA algorithm and PCPA algorithm, respectively. The snapshot number is 300 and the SNR is 0dB. As it can be seen in Figure 3, all these algorithms can obtain the correct estimation results of DOA angle β under the condition that the incident signals are more than array sensors. However, the PCPA algorithm and the TPCPA algorithm have larger estimation bias than the proposed algorithm, and there are more visible pseudo-peaks in the spatial spectrum. This certifies the

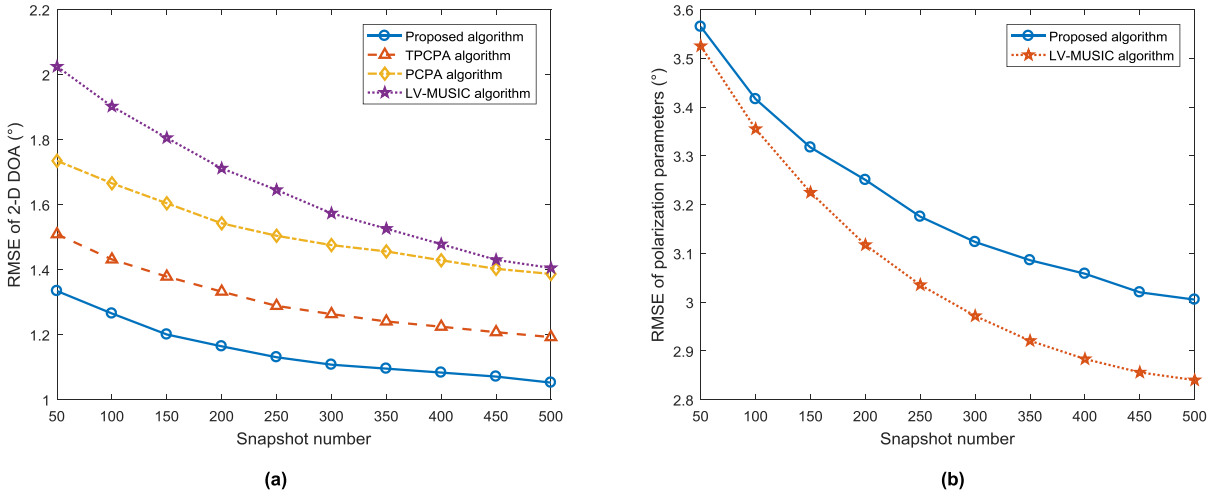

FIGURE 5. The RMSEs of (a) 2-D DOA angles and (b) polarization parameters versus snapshot number with SNR=0dB.

effectiveness of the proposed algorithm on the underdetermined condition.

In the second simulation, we discuss the parameter estimation accuracy versus SNR. Consider $K = 4$ far-field narrowband signals, and the DOA angels and polarization parameters $(\alpha, \beta, \gamma, \eta)$ are (115°, 35°, 27°, 52°), (50°, 65°, 42°, −49°), (70°, 130°, −43°, −86°), and (100°, 150°, 41°, 73°), respectively. The regularization parameter μ is set as 1 for the TPCPA algorithm and PCPA algorithm. The searching step of LV-MUSIC algorithm in 2-D spatial domain and the interval of uniform spatial grid in β angle domain for other algorithms are both 0.1°. The SNR varies from −10dB to 20dB with the step size 5dB, and the snapshot number is fixed to 300. The RMSEs are obtained by performing 300 independent trials. As it can be seen in the Figure 4, the RMSEs of estimated parameters all decrease with the increase of SNR. Since the new cross-covariance matrix without the polarization parameters is constructed, the proposed algorithm outperforms than the other algorithms. The extended DOF would also intensity the trend. When the SNR is low, the orthogonality of the signal- and noise-subspace in the LV-MUSIC algorithm is affected, leading to an increase of the RMSE than SR-based algorithms.

Moreover, it can be seen that although the proposed algorithm has better DOA estimation accuracy than LV-MUSIC algorithm, the RMSE of the polarization parameters is better. The main reason is that the proposed algorithm estimates the polarization parameters based on the DOA estimation results. The DOA estimation deviation would cause more estimation bias in the process of polarization parameter estimation. This would not appear in the LV-MUSIC algorithm.

Then, we evaluate the estimation accuracy of the parameters versus snapshot number, as shown in the Figure 5. The snapshot number varies from 50 to 500 with the step size 50, and the SNR is fixed to 0dB. The other conditions are same with that in the second simulation. Similar to the RMSE curves versus SNR, the RMSEs of parameters decreases with the increase of snapshots, and the proposed algorithm outperforms than the other algorithms. In addition, it can be seen that the subspace-based algorithm i.e., LV-MUSIC algorithm is more affected by the snapshots than the SR-based algorithms.

VI. CONCLUSIONS

In this paper, a novel 2-D DOA and polarization parameter estimation algorithm based on three-parallel co-prime polarization sensitive array has been proposed. The reconstructed cross-covariance matrix not containing polarization information is used, so that the estimation of 2-D DOA angles and polarization parameters can be decoupled. Through vectorization operation and linear transformation, a virtual ULA containing more elements is constructed. In so doing, the DOFs of the array increase and more targets can be detected with limited number of physical sensors. The sparse representation based estimation method is presented to estimate 2-D DOA with only 1-D overcomplete dictionary, which reduces the computational complexity dramatically. Meanwhile, the constraint form of the optimization problem based on the upper bound of the data fitting error is derived to avoid the selection of the regularization parameter. Finally, the data vectors are constructed by using the cross-covariance matrix between different components of the received array data, and the polarization parameters are estimated via least squares method. Since the co-prime structure is applied to PSA, the DOFs of the array are extended, and due to the sparse placement of sensors, the array aperture is increased and the mutual coupling is weakened. From the simulation results, it can be seen that these advantages make the proposed algorithm can solve the underdetermined estimation problem and have better estimation accuracy.

APPENDIX

In the appendix, we discuss the calculations of mean and variance of $\Delta \boldsymbol{r}_{\varsigma}$. For convenience, the component symbol ς is omitted here in the equations. But please remember that the following derivations are only for one component.

First compute the mean of $\Delta \boldsymbol{r}$. Since

$$\begin{aligned} E\left\{\hat{\boldsymbol{R}}\right\} &= E\left\{[\hat{\boldsymbol{R}}_{31}\ \hat{\boldsymbol{R}}_{12}]\right\} \\ &= \left[E\left\{\hat{\boldsymbol{R}}_{31}\right\}\ E\left\{\hat{\boldsymbol{R}}_{12}\right\}\right] \\ &= [\boldsymbol{R}_{31}\ \boldsymbol{R}_{12}] = \boldsymbol{R}, \end{aligned} \tag{66}$$

the mean of $\Delta \boldsymbol{r}$ is 0.

Then compute the variance of $\Delta \boldsymbol{r}$. The variance of $\Delta \boldsymbol{r}$ can be expressed as

$$\begin{aligned} \boldsymbol{C} &= E\left[\Delta \boldsymbol{r} \Delta \boldsymbol{r}^{\mathrm{H}}\right] \\ &= E\begin{bmatrix} \Delta \boldsymbol{r}_{31}\Delta \boldsymbol{r}_{31}^{\mathrm{H}} & \Delta \boldsymbol{r}_{31}\Delta \boldsymbol{r}_{12}^{\mathrm{H}} \\ \Delta \boldsymbol{r}_{12}\Delta \boldsymbol{r}_{31}^{\mathrm{H}} & \Delta \boldsymbol{r}_{12}\Delta \boldsymbol{r}_{12}^{\mathrm{H}} \end{bmatrix}. \end{aligned} \tag{67}$$

In accordance with [25], the variance of $\Delta \boldsymbol{r}_{31}$ and $\Delta \boldsymbol{r}_{12}$ are

$$E\left[\Delta \boldsymbol{r}_{12}\Delta \boldsymbol{r}_{12}^{\mathrm{H}}\right] = \frac{1}{L}\boldsymbol{R}_2^{\mathrm{T}} \otimes \boldsymbol{R}_1, \tag{68}$$

$$E\left[\Delta \boldsymbol{r}_{31}\Delta \boldsymbol{r}_{31}^{\mathrm{H}}\right] = \frac{1}{L}\boldsymbol{R}_1^{\mathrm{T}} \otimes \boldsymbol{R}_3. \tag{69}$$

Following the ideas, we drive the expressions of $E[\Delta \boldsymbol{r}_{12}\Delta \boldsymbol{r}_{31}^{\mathrm{H}}]$ and $E[\Delta \boldsymbol{r}_{12}\Delta \boldsymbol{r}_{31}^{\mathrm{H}}]$. The i-th column of the cross-covariance matrix between subarray 1 and 2 and that between subarray 3 and 1 are

$$\hat{\boldsymbol{r}}_{12,i} = \frac{1}{L}\sum_{t=1}^{L} \boldsymbol{x}_1(t)\left(x_{2,i}(t)\right)^*, \tag{70}$$

$$\hat{\boldsymbol{r}}_{31,i} = \frac{1}{L}\sum_{t=1}^{L} \boldsymbol{x}_3(t)\left(x_{1,i}(t)\right)^* \tag{71}$$

where $x_{2,i}(t)$ and $x_{1,i}(t)$ are the i-th entry of $\boldsymbol{x}_2(t)$ and $\boldsymbol{x}_1(t)$, respectively. Then we can get

$$\begin{aligned} &E\left[\hat{\boldsymbol{r}}_{12,i}\hat{\boldsymbol{r}}_{31,j}^{\mathrm{H}}\right] \\ &= \frac{1}{L^2}\sum_{t=1}^{L}\sum_{p=1}^{L} E\left[\boldsymbol{x}_1(t)\left(x_{2,i}(t)\right)^*\left(\boldsymbol{x}_3(p)\right)^{\mathrm{H}} x_{1,j}(p)\right] \\ &= \frac{1}{L^2}\sum_{t=1}^{L} E\left[\boldsymbol{x}_1(t)\left(x_{2,i}(t)\right)^*\right] \sum_{p=1,p\neq t}^{L} E\left[\left(\boldsymbol{x}_3(p)\right)^{\mathrm{H}} x_{1,j}(p)\right] \\ &\quad + \frac{1}{L^2}\sum_{t=1}^{L} E\left[\boldsymbol{x}_1(t)\left(x_{2,i}(t)\right)^*\left(\boldsymbol{x}_3(t)\right)^{\mathrm{H}} x_{1,j}(t)\right] \\ &= \boldsymbol{r}_{12,i}\boldsymbol{r}_{31,j}^{\mathrm{H}} + \frac{1}{L}R_{12,ji}\boldsymbol{R}_{13}. \end{aligned} \tag{72}$$

According to (66) we have $E[\hat{\boldsymbol{r}}_{12}] = \boldsymbol{r}_{12}$ and $E[\hat{\boldsymbol{r}}_{31}] = \boldsymbol{r}_{31}$, then the cross-covariance matrix of $\Delta \boldsymbol{r}_{12}$ and $\Delta \boldsymbol{r}_{31}$ is

$$\begin{aligned} E\left[\Delta \boldsymbol{r}_{12}\Delta \boldsymbol{r}_{31}^{\mathrm{H}}\right] &= E\left[(\hat{\boldsymbol{r}}_{12} - \boldsymbol{r}_{12})(\hat{\boldsymbol{r}}_{31} - \boldsymbol{r}_{31})^{\mathrm{H}}\right] \\ &= E[\hat{\boldsymbol{r}}_{12}\hat{\boldsymbol{r}}_{31}^{\mathrm{H}}] - \boldsymbol{r}_{12}\boldsymbol{r}_{31}^{\mathrm{H}} \\ &= \frac{1}{L}\begin{bmatrix} R_{12,11}\boldsymbol{R}_{13} & \cdots & R_{12,1N}\boldsymbol{R}_{13} \\ \vdots & \ddots & \vdots \\ R_{12,N1}\boldsymbol{R}_{13} & \cdots & R_{12,NN}\boldsymbol{R}_{13} \end{bmatrix} \\ &= \frac{1}{L}\boldsymbol{R}_{12}^{\mathrm{T}} \otimes \boldsymbol{R}_{13}. \end{aligned} \tag{73}$$

Similarly, it can be derived that

$$E\left[\hat{\boldsymbol{r}}_{31,i}\hat{\boldsymbol{r}}_{12,j}^{\mathrm{H}}\right] = \boldsymbol{r}_{31,i}\boldsymbol{r}_{12,j}^{\mathrm{H}} + \frac{1}{L}R_{21,ji}\boldsymbol{R}_{31}, \tag{74}$$

and

$$E\left[\Delta \boldsymbol{r}_{31}\Delta \boldsymbol{r}_{12}^{\mathrm{H}}\right] = \frac{1}{L}\boldsymbol{R}_{21}^{\mathrm{T}} \otimes \boldsymbol{R}_{31}. \tag{75}$$

Therefore, the variance of the estimation error of $\Delta \boldsymbol{r}$ is

$$\begin{aligned} C &= E\left[\Delta \boldsymbol{r}\Delta \boldsymbol{r}^{\mathrm{H}}\right] \\ &= E\begin{bmatrix} \Delta \boldsymbol{r}_{31}\Delta \boldsymbol{r}_{31}^{\mathrm{H}} & \Delta \boldsymbol{r}_{31}\Delta \boldsymbol{r}_{12}^{\mathrm{H}} \\ \Delta \boldsymbol{r}_{12}\Delta \boldsymbol{r}_{31}^{\mathrm{H}} & \Delta \boldsymbol{r}_{12}\Delta \boldsymbol{r}_{12}^{\mathrm{H}} \end{bmatrix} \\ &= \frac{1}{L}\begin{bmatrix} \boldsymbol{R}_1^{\mathrm{T}} \otimes \boldsymbol{R}_3 & \boldsymbol{R}_{21}^{\mathrm{T}} \otimes \boldsymbol{R}_{31} \\ \boldsymbol{R}_{12}^{\mathrm{T}} \otimes \boldsymbol{R}_{13} & \boldsymbol{R}_2^{\mathrm{T}} \otimes \boldsymbol{R}_1 \end{bmatrix}. \end{aligned} \tag{76}$$

ACKNOWLEDGMENT

The authors would like to thank the anonymous reviewers for their valuable comments and suggestions.

REFERENCES

[1] L. Wan, G. Han, J. Jiang, C. Zhu, and L. Shu, "A DOA estimation approach for transmission performance guarantee in D2D communication," *Mobile Netw. Appl.*, vol. 22, no. 6, pp. 998–1009, 2017.
[2] L. Wan, X. Kong, and F. Xia, "Joint range-Doppler-angle estimation for intelligent tracking of moving aerial targets," *IEEE Internet Things J.*, vol. 5, no. 3, pp. 1625–1636, Jun. 2018.
[3] P. Zhao, W. Si, G. Hu, and L. Wang, "DOA estimation for a mixture of uncorrelated and coherent sources based on hierarchical sparse Bayesian inference with a gauss-exp-chi^2 prior," *Int. J. Antennas Propag.*, vol. 2018, Jul. 2018, Art. no. 3505918.
[4] G. Zheng, "Two-dimensional DOA estimation for polarization sensitive array consisted of spatially spread crossed-dipole," *IEEE Sensors J.*, vol. 18, no. 12, pp. 5014–5023, Jun. 2018.
[5] K. T. Wong, Y. Song, C. J. Fulton, S. Khan, and W.-Y. Tam, "Electrically 'long' dipoles in a collocated/orthogonal triadâĂŤfor direction finding and polarization estimation," *IEEE Trans. Antennas Propag.*, vol. 65, no. 11, pp. 6057–6067, Nov. 2017.
[6] W. Si, Y. Wang, and C. Zhang, "2D-DOA and polarization estimation using a novel sparse representation of covariance matrix with COLD array," *IEEE Access*, vol. 6, pp. 66385–66395, 2018.
[7] J. Dai, X. Xu, and D. Zhao, "Direction-of-arrival estimation via real-valued sparse representation," *IEEE Antennas Wireless Propag. Lett.*, vol. 12, pp. 376–379, 2013.
[8] J. Yin and T. Chen, "Direction-of-arrival estimation using a sparse representation of array covariance vectors," *IEEE Trans. Signal Process.*, vol. 59, no. 9, pp. 4489–4493, Sep. 2011.
[9] W. Si, Y. Wang, C. Hou, and H. Wang, "Real-valued 2D MUSIC algorithm based on modified forward/backward averaging using an arbitrary centrosymmetric polarization sensitive array," *Sensors*, vol. 17, no. 10, pp. 2241–2256, Oct. 2017.
[10] E. Ferrara, Jr., and T. Parks, "Direction finding with an array of antennas having diverse polarizations," *IEEE Trans. Antennas Propag.*, vol. 31, no. 2, pp. 231–236, Mar. 1983.
[11] X. Zhang, C. Chen, J. Li, and D. Xu, "Blind DOA and polarization estimation for polarization-sensitive array using dimension reduction MUSIC," *Multidimensional Syst. Signal Process.*, vol. 25, no. 1, pp. 67–82, Apr. 2012.
[12] K. T. Wong and M. D. Zoltowski, "Self-initiating MUSIC-based direction finding and polarization estimation in spatio-polarizational beamspace," *IEEE Trans. Antennas Propag.*, vol. 48, no. 8, pp. 1235–1245, Aug. 2000.
[13] K. T. Wong and M. D. Zoltowski, "Uni-vector-sensor ESPRIT for multisource azimuth, elevation, and polarization estimation," *IEEE Trans. Antennas Propag.*, vol. 45, no. 10, pp. 1467–1474, Oct. 1997.

[14] K. T. Wong and M. D. Zoltowski, "Closed-form direction finding and polarization estimation with arbitrarily spaced electromagnetic vector-sensors at unknown locations," *IEEE Trans. Antennas Propag.*, vol. 48, no. 5, pp. 671–681, May 2000.
[15] A. Nehorai and E. Paldi, "Vector-sensor array processing for electromagnetic source localization," *IEEE Trans. Signal Process.*, vol. 42, no. 2, pp. 376–398, Feb. 1994.
[16] K.-T. Wong and X. Yuan, "'Vector cross-product direction-finding' with an electromagnetic vector-sensor of six orthogonally oriented but spatially noncollocating dipoles/loops," *IEEE Trans. Signal Process.*, vol. 59, no. 1, pp. 160–171, Jan. 2011.
[17] F. Luo and X. Yuan, "Enhanced 'vector-cross-product' direction-finding using a constrained sparse triangular-array," *EURASIP J. Adv. Signal Process.*, vol. 2012, no. 1, pp. 1–11, Dec. 2012.
[18] C.-L. Liu and P. P. Vaidyanathan, "Super nested arrays: Linear sparse arrays with reduced mutual coupling—Part I: Fundamentals," *IEEE Trans. Signal Process.*, vol. 64, no. 15, pp. 3997–4012, Apr. 2016.
[19] W. Si, Z. Peng, C. Hou, and F. Zeng, "Two-dimensional DOA estimation for three-parallel nested subarrays via sparse representation," *Sensors*, vol. 18, no. 6, pp. 1861–1866, Jun. 2018.
[20] P. P. Vaidyanathan and P. Pal, "Sparse sensing with co-prime samplers and arrays," *IEEE Trans. Signal Process.*, vol. 59, no. 2, pp. 573–586, Feb. 2011.
[21] S. Qin, Y. D. Zhang, and M. G. Amin, "Generalized coprime array configurations for direction-of-arrival estimation," *IEEE Trans. Signal Process.*, vol. 63, no. 6, pp. 1377–1390, Mar. 2015.
[22] W. Chang, J. Ru, and L. Deng, "Stokes parameters and DOA estimation of polarised sources with unknown number of sources," *IET Radar Sonar Navigat.*, vol. 12, no. 2, pp. 218–226, Feb. 2018.
[23] W. Si, F. Zeng, C. Hou, and Z. Peng, "A sparse-based off-grid DOA estimation method for coprime arrays," *Sensors*, vol. 18, no. 6, pp. 3025–3040, Sep. 2018.
[24] Z. Cheng, Y. Zhao, H. Li, and P. Shui, "Two-dimensional DOA estimation algorithm with co-prime array via sparse representation," *Electron. Lett.*, vol. 51, no. 25, pp. 2084–2086, Dec. 2015.
[25] J. Li, D. Jiang, and X. Zhang, "Sparse representation based two-dimensional direction of arrival estimation using co-prime array," *Multidimensional Syst. Signal Process.*, vol. 29, no. 1, pp. 35–47, Sep. 2016.
[26] F. Sun, P. Lan, B. Gao, and G. Zhang, "An efficient dictionary learning-based 2-D DOA estimation without pair matching for co-prime parallel arrays," *IEEE Access*, vol. 6, pp. 8510–8518, 2018.
[27] P. Gong, X.-F. Zhang, J. Shi, and W. Zheng, "Three-parallel co-prime array configuration for two-dimensional DOA estimation," in *Proc. WCSP*, Nanjing, China, Oct. 2017, pp. 1–5.
[28] Q. Wu, F. Sun, P. Lan, G. Ding, and X. Zhang, "Two-dimensional direction-of-arrival estimation for co-prime planar arrays: A partial spectral search approach," *IEEE Sensors J.*, vol. 16, no. 14, pp. 5660–5670, Jul. 2016.
[29] J. Shi, G. Hu, X. Zhang, F. Sun, and H. Zhou, "Sparsity-based two-dimensional DOA estimation for coprime array: From sum–difference coarray viewpoint," *IEEE Trans. Signal Process.*, vol. 65, no. 21, pp. 5591–5604, Nov. 2017.
[30] P. P. Vaidyanathan and P. Pal, "Theory of sparse coprime sensing in multiple dimensions," *IEEE Trans. Signal Process.*, vol. 59, no. 8, pp. 3592–3608, Aug. 2011.
[31] P. Pal and P. P. Vaidyanathan, "Coprime sampling and the music algorithm," in *Proc. DSP/SPE*, Sedona, AZ, USA, Jan. 2011, pp. 289–294.
[32] Z. Tan, Y. C. Eldar, and A. Nehorai, "Direction of arrival estimation using co-prime arrays: A super resolution viewpoint," *IEEE Trans. Signal Process.*, vol. 62, no. 21, pp. 5565–5576, Nov. 2014.
[33] C. L. Liu and P. P. Vaidyanathan, "Remarks on the spatial smoothing step in coarray Music," *IEEE Signal Process. Lett.*, vol. 22, no. 9, pp. 1438–1442, Sep. 2015.
[34] Y. Tian, X. Sun, and S. Zhao, "Sparse-reconstruction-based direction of arrival, polarisation and power estimation using a cross-dipole array," *IET Radar Sonar Navigat.*, vol. 9, no. 6, pp. 727–731, Jul. 2015.
[35] J. Li, Y. Li, and X. Zhang, "Two-dimensional off-grid DOA estimation using unfolded parallel coprime array," *IEEE Commun. Lett.*, vol. 22, no. 12, pp. 2495–2498, Dec. 2018.
[36] A. Liu, Q. Yang, X. Zhang, and W. Deng, "Direction-of-arrival estimation for coprime array using compressive sensing based array interpolation," *Int. J. Antennas Propag.*, vol. 2017, Feb. 2017, Art. no. 6425067.
[37] W.-X. Chang, X.-B. Li, and J. Wang, "Stokes parameters and 2-D DOAs estimation of polarized sources with an L-shaped coprime array," *Digit. Signal Process.*, vol. 78, pp. 30–41, Jul. 2018.
[38] D. Malioutov, M. Çetin, and A. S. Willsky, "A sparse signal reconstruction perspective for source localization with sensor arrays," *IEEE Trans. Signal Process.*, vol. 53, no. 8, pp. 3010–3022, Aug. 2005.
[39] Z.-Q. He, Z.-P. Shi, and L. Huang, "Covariance sparsity-aware DOA estimation for nonuniform noise," *Digit. Signal Process.*, vol. 28, pp. 75–81, May 2014.
[40] F. Alizadeh and D. Goldfarb, "Second-order cone programming," *Math. Program.*, vol. 95, no. 1, pp. 3–51, Jan. 2003.

WEIJIAN SI was born in Beijing, China, in 1971. He received the B.E. degree from Beihang University, in 1994, and the Ph.D. degree from Harbin Engineering University, Heilongjiang, China, in 2004. From 1995 to 1999, he joined the 35th Institute of China Aerospace Science and Industry Corporation, where he was engaged in scientific research on radar signal processing. He is currently a Professor and a Ph.D. Supervisor with the College of Information and Communication Engineering, Harbin Engineering University. His main research interests include radar signal detection, processing and identification, high-precision passive direction finding, and spatial spectrum estimation.

YAN WANG was born in Pingdingshan, China, in 1992. He received the B.E. degree in electronic information engineering from Harbin Engineering University, Heilongjiang, China, in 2013, where he is currently pursuing the Ph.D. degree in information and communication engineering. His research interests include high-precision passive direction finding and its applications.

CHUNJIE ZHANG was born in Heilongjiang, China, in 1975. She received the B.E. and Ph.D. degrees from Harbin Engineering University, Heilongjiang, in 2004 and 2006, respectively, where she is currently an Associate Professor with the College of Information and Communication Engineering. Her main research interests include wideband channelized receivers, pulse compression signal processing, and microwave spectrum analysis based on the photonic signal processing.